

## Dissipative Chaos in Quantum Distributions

T. V. GEVORGYAN<sup>1,\*</sup>, S. B. MANVELYAN<sup>1</sup>

<sup>1</sup>*Institute for Physical Researches, National Academy of Sciences,  
Ashtarak-2, 0203, Ashtarak, Armenia*

*\*E-mail: t.gevorgyan@ysu.am  
www.ipr.sci.am*

A. R. SHAHINYAN<sup>2,\*\*</sup>, G. Yu. KRYUCHKYAN<sup>1,2,\*\*\*</sup>

<sup>2</sup>*Yerevan State University, A. Manoogian 1, 0025, Yerevan, Armenia*

*\*\*E-mail: anna\_shahinyan@ysu.am, \*\*\*E-mail: kryuchkyan@ysu.am  
www.ysu.am*

We discuss some problems of dissipative chaos for open quantum systems in the framework of semiclassical and quantum distributions. For this goal, we propose a driven nonlinear oscillator with time-dependent coefficients, i.e. with time-dependent Kerr-nonlinearity and time-modulated driving field. This model showing both regular and chaotic dynamics in the classical limit is realized in several experimental schemes. Quantum dissipative chaos is analyzed on the base of numerical method of quantum trajectories. Three quantities are studied: the Wigner function of oscillatory mode from the point of view of quantum-assemble theory and both semiclassical Poincaré section and quantum Poincaré section calculated on a single quantum trajectory. The comparative analysis of these distributions for various operational chaotic regimes of the models is performed, as well as scaling invariance in dissipative chaos and quantum interference effects assisted by chaos are discussed.

*Keywords:* Quantum optics, Nonlinear dynamics

### 1. Introduction

Quantum nonlinear systems with chaotic classical counterparts have received much attention in the last two decades. This field of investigation is sometimes called quantum chaos<sup>1</sup>. The majority of studies of quantum chaos for isolated or so-called Hamiltonian systems, the classical counterparts of which are chaotic, focus on static properties such as spectral statistics of energy levels and transition probabilities between eigenstates of the system. A variety of studies have also been carried out to understand the

features of time-dependent chaotic systems. In contrast to that very little work has been done to investigate quantum chaos for open nonlinear systems. The beginning of study of an open chaotic system can be dated back to the papers<sup>2</sup> where the authors have analyzed the kicked rotor and similar systems with discrete time interacting with a heat bath. Quite generally, chaos in classical conservative and dissipative systems with noise has completely different properties, e.g., strange attractors can appear only in dissipative systems. For dissipative systems Poincaré section has form of strange attractor in phase space while for Hamiltonian systems it has form of close contours with separatrices.

In classical mechanics a standard characterization of chaos might be given in terms of the unpredictability of phase-space trajectories or Poincaré section that consists of non-localized distributed points. However, the most important characteristic of classical chaotic systems-exponential divergence of trajectories, starting at arbitrarily close initial points in phase space does not have quantum counterpart because of the Hiesenberg uncertainty principle. The question has been posed of what constitutes the quantum mechanical equivalent of chaos. Many criteria have been suggested to define chaos in quantum systems, varying in their emphasis and domain of application<sup>1, 3</sup>. As yet, there is no universally accepted definition of quantum chaos.

In recent years much effort has been expended, both theoretically and experimentally, to explore the role of quantum fluctuations and noise in the order-to-chaos transition for open systems. It is obvious that the investigations in this area are connected with the quantum-classical correspondence problem, in general, and with the environment induced decoherence and dissipation, in particular. Recently, this topic has been the focus of theoretical investigations. As a part of these studies, it has been recognized<sup>4</sup> that the decoherence has rather unique properties for systems classical analogs of which are chaotic. In particular, the formation of sub-Planck structure in phase space has been discussed for chaotic system<sup>5</sup>. The connection between quantum and classical treatments of chaos was also realized by means of comparison between strange attractors on the classical Poincaré section and the contour plots of the Wigner functions<sup>10</sup>.

In this paper we investigate some problems of dissipative chaos for open quantum systems in the framework of quantum distributions. We use the traditional ensemble description of Markovian open systems, based on the master equation. This equation is presented in quantum trajectories in the framework of the quantum state diffusion approach<sup>6</sup>. Recently, it was shown

how quantum state diffusion can be used to model dissipative chaotic systems on individual quantum trajectories<sup>7, 8</sup>. In contrast with these papers, here we show that it is possible to describe quantum chaos using also a statistical ensemble of trajectories, which is actually realized in nature.

The requirement in realization of this study is to have a proper quantum model showing both regular and chaotic dynamics in the classical limit. We propose a driven nonlinear oscillator with time-dependent coefficients for this goal. This model proposed to study the quantum chaos in the series of papers<sup>9, 11, 10, 12, 13</sup> allow us to examine challenging problems of quantum dissipative chaos, including the problem of the quantum counterpart of a strange attractor.

The other problem of our interest in this paper relates to the quantum effects in systems with chaotic dynamics. Particularly, in a recent paper, sub-Poissonian statistics of oscillatory excitations numbers was established for chaotic dynamics of nonlinear oscillator<sup>11</sup>. It was shown that quantum-interference phenomena can be realized for the dissipative nonlinear systems exhibiting hysteresis-cycle behavior and quantum chaos<sup>10, 12, 13</sup>. The study of these phenomena provides a fundamental understanding of quantum fluctuations in quantum chaos and opens a way for new experimental studies of the quantum dissipative chaos in the field of quantum optics.

The outline of this paper is as follows. In Sec.II we describe both the model and the method of calculations. In Sec. III we analyze correspondence between Poincaré sections and Wigner functions for the chaotic dynamics. In Sec. IV we analyze scaling invariance for quantum system and discuss quantum chaos for the regimes in which the classical chaos is lost. In Sec.V we present results on quantum interference phenomena for chaotic dynamics. We summarize our results in Sec.VI.

## 2. Driven nonlinear oscillator as an open quantum system

In this section the systems and the methods of calculations are presented. We treat the Duffing oscillator as an open quantum system and assume that its time evolution is described by Markovian dynamics in terms of the Lindblad master equation for the reduced density matrix  $\rho$ . In the interaction picture that corresponds to the transformation  $\rho \longrightarrow e^{-i\omega a^\dagger at} \rho e^{i\omega a^\dagger at}$ , where  $a^\dagger$  and  $a$  are the Bose annihilation and creation operators of the os-

cillatory mode and  $\omega$  is the driving frequency, this equation reads as

$$\frac{d\rho}{dt} = \frac{-i}{\hbar}[H_0 + H_{int}, \rho] + \sum_{i=1,2} \left( L_i \rho L_i^\dagger - \frac{1}{2} L_i^\dagger L_i \rho - \frac{1}{2} \rho L_i^\dagger L_i \right). \quad (1)$$

The Hamiltonians are

$$\begin{aligned} H_0 &= \hbar \Delta a^\dagger a, \\ H_{int} &= \hbar \chi(t) (a^\dagger a)^2 + \hbar (f(t) a^\dagger + f(t)^* a), \end{aligned} \quad (2)$$

where  $\chi(t)$  and  $f(t)$ , which may or may not depend on time, represent, respectively, the strength of the nonlinearity and amplitude of the force,  $\omega_0$  is the resonant frequency,  $\Delta = \omega_0 - \omega$  is the detuning. The dissipative and decoherence effects, losses, and thermal noise are included in the last part of the master equation, where  $L_i$  are the Lindblad operators:

$$L_1 = \sqrt{(N+1)\gamma} a, \quad L_2 = \sqrt{N\gamma} a^\dagger, \quad (3)$$

$\gamma$  is the spontaneous decay rate of the dissipation process and  $N$  denotes the mean number of quanta of a heat bath. Here we focus on the pure quantum effects and assume  $N = 0$ .

This model seems experimentally feasible and can be realized in several experimental schemes. In fact, a single mode e.m. field is well described in terms of an anharmonic oscillator (AHO), and the nonlinear medium could be an optical fiber or a  $\chi(3)$  crystal, placed in a cavity. The anharmonicity of mode dynamics comes from the self-phase modulation due to the photon-photon interaction in the  $\chi(3)$  medium. In this case, it is possible to realize time modulation of the strength of the nonlinearity by using a media with periodic variation of the  $\chi(3)$  susceptibility.

On the other side, the Hamiltonian described by Eq. (2) describes a single nanomechanical resonator with  $a^\dagger$  and  $a$  raising and lowering operators related to the position and momentum operators of a mode quantum motion

$$x = \sqrt{\frac{\hbar}{2m\omega_0}} (a + a^\dagger), \quad p = -i\sqrt{2\hbar m\omega_0} (a - a^\dagger),$$

where  $m$  is the effective mass of the nanomechanical resonator,  $\omega_0$  is the linear resonator frequency and  $\chi$  proportional to the Duffing nonlinearity. One of the variants of nano-oscillators is based on a double-clamped platinum beam<sup>14</sup> for which the nonlinearity parameter equals to  $\chi = \hbar/4\sqrt{3}Qma_c^2$ , where  $a_c$  is the critical amplitude at which the resonance amplitude has

an infinite slope as a function of the driving frequency,  $Q$  is the mechanical quality factor of the resonator. In this case, the giant nonlinearity  $\chi \cong 3.4 \cdot 10^{-4} \text{s}^{-1}$  was realized. Note, that details of this resonator, including the expression for the parameter  $a_c$ , are presented in<sup>15</sup>. On decreasing nanomechanical resonator mass, its resonance frequency increases, exceeding 1 GHz in recent experiments<sup>16, 17</sup>. It is possible to reach a quantum regime for such frequencies, i.e., to cool down the temperatures for which thermal energy will be comparable to the energy of oscillatory quanta. The recent investigations in this direction are devoted to classical to quantum transition of a driven nanomechanical oscillator<sup>18</sup>, generation of Fock states<sup>19</sup>, nonlinear dynamics, and stochastic resonance<sup>20</sup>. Note, that in the last few years there has been rapid progress in the construction and manipulation of such nanomechanical oscillators with giant  $\chi(3)$ -Kerr nonlinearity. The nanomechanical resonator with a significant fourth-order nonlinearity in the elastic potential energy has been experimentally demonstrated<sup>21</sup>. It has also been shown that this system is dynamically equivalent to the Duffing oscillator with varied driving force<sup>22</sup>. This scheme is widely employed for a large variety of applications as well as the other schemes of micro- and nanomechanical oscillators, more commonly as sensors or actuators in integrated electrical, optical, and optoelectrical systems<sup>16, 23</sup>.

Cyclotron oscillations of a single electron in a Penning trap with a magnetic field are another realization of the quantum version of the Duffing oscillator<sup>24, 25, 26</sup>. In this case the anharmonicity comes from the nonlinear effect that is caused by the relativistic motion of an electron in a trap, while the dissipation effects arise from the spontaneous emission of the synchrotron radiation and thermal fluctuations of the cyclotron motion. Note that a one-electron oscillator allows one to achieve a relatively strong cubic nonlinearity,  $\chi/\gamma \lesssim 1$ .

In recent years the study of quantum dynamics of oscillators with time-dependent parameters has been focus of considerable attention. This interest is justified by many applications in different contexts. Particular, one application concerns to the center of mass motion of a laser cooled and trapped ion in a Paul trap<sup>27</sup>. The quantum dynamics of an AHO with time dependent modulation of its frequency and nonlinearity parameters has been investigated in applications to macroscopic superposition of quantum states<sup>28</sup>.

It is well assessed that in the case of unitary dynamics, without any losses, an anharmonic oscillator leads to sub-Poissonian statistics of oscillatory excitation number, quadratic squeezing and superposition of macro-

scopically distinguishable coherent states. For dissipative dynamics the important parameter responsible for production of nonclassical states via  $\chi(3)$  materials is the ratio between nonlinearity and damping. Therefore, the practical realization of such quantum effects requires a high nonlinearity with respect to dissipation. In this direction the largest nonlinear interaction was proposed in many papers, particularly, in terms of electromagnetically induced transparency<sup>29</sup> and by using the Purcell effect<sup>30</sup>, and in cavity QED<sup>31</sup>. The significant nonlinearity has also been observed for nanomechanical resonators<sup>14</sup>. These methods can lead to  $\chi(3)$  nonlinearity of several orders of magnitude higher than natural optical self-Kerr interactions. Note, that high  $\chi(3)$  nonlinear oscillators generate also a lot of interest recently due to their applications in areas of quantum computing<sup>32</sup>.

In the case of nonlinear dissipative  $\chi(3)$  interaction stimulated by coherent driving force, the time evolution cannot be solved analytically for arbitrary evolution times and suitable numerical methods have to be used. Nevertheless, with dissipation included a driven AHO model has been solved exactly in the steady-state regime in terms of the Fokker-Planck equation in the complex P representation<sup>33</sup>. Analogous solution has been obtained for a combined driven parametric oscillator with Kerr nonlinearity<sup>34</sup>. The Wigner functions for both these models have been obtained using these solutions<sup>33, 35</sup>.

The investigation of quantum dynamics of a driven dissipative nonlinear oscillator for non-stationary cases is much more complicated and only a few papers have been done in this field up to now. More recently, the quantum version of dissipative AHO or the Duffing oscillator with time-modulated driving force has been studied in the series of the papers<sup>7</sup> in the context of a stochastic resonance<sup>9</sup>, quantum-to-classical transition and investigation of quantum dissipative chaos<sup>10, 11</sup>.

For the constant parameters  $\chi(t) = \chi$  and  $f(t) = f$  the equations (1) and (2) describe the model of a driven dissipative AHO that was introduced long ago in quantum optics to describe bistability due to a Kerr nonlinear medium<sup>36</sup>. For the case of time-dependent parameters  $\chi(t)$  and  $f(t)$  the dynamics of the AHO exhibits a rich phase-space structure, including regimes of regular, bistable and chaotic motion. We perform our calculations for regular and chaotic regimes concerning two models of time-modulated AHO corresponding to two physical situations: (i)  $\chi = \chi(t) = \chi_0 + \chi_1 \sin(\Omega t)$  and  $f(t) = \text{const} = f$ ; (ii)  $f = f(t) = f_0 + f_1 \exp(\delta t)$  and  $\chi(t) = \text{const} = \chi$  with  $\delta \ll \omega$  and  $\Omega \ll \omega$  are the modulation frequencies.

We analyze the master equation numerically using quantum state dif-

fusion method (QSD)<sup>6</sup>. According to this method, the reduced density operator is calculated as an ensemble mean

$$\rho(t) = M(|\psi_\xi(t)\rangle\langle\psi_\xi(t)|) = \lim_{N \rightarrow \infty} \frac{1}{N} \sum_{\xi}^N |\psi_\xi(t)\rangle\langle\psi_\xi(t)| \quad (4)$$

over the stochastic pure states  $|\psi_\xi(t)\rangle$  describing evolution along a quantum trajectory. The stochastic equation for the state  $|\psi_\xi(t)\rangle$  involves both Hamiltonian described by Eq. (2) and the Lindblad operators described by Eq. (3) and reads as:

$$|d\Psi_\xi\rangle = -\frac{i}{\hbar}H|\Psi_\xi\rangle dt - \frac{1}{2} \sum_{i=1,2} (L_i^\dagger L_i - 2\langle L_i^\dagger \rangle L_i + \langle L_i \rangle \langle L_i^\dagger \rangle) |\Psi_\xi\rangle dt + \sum_{i=1,2} (L_i - \langle L_i \rangle) |\Psi_\xi\rangle d\xi, \quad (5)$$

where  $\xi$  is the generated complex gaussian noise that satisfies the following conditions:

$$M(d\xi_i) = 0, M(d\xi_i d\xi_j) = 0, M(d\xi_i d\xi_j^*) = \delta_{ij} dt. \quad (6)$$

We calculate the density operator using an expansion of the state vector  $|\psi_\xi\rangle$  in a truncated basis of Fock's number states of a harmonic oscillator

$$|\psi_\xi(t)\rangle = \sum_n a_n^\xi(t) |n\rangle. \quad (7)$$

### 3. Wigner function and Poincaré section

In this section we shortly examine correspondence between the Poincaré section and the Wigner function of the oscillatory mode considering the model (ii) with time-dependent driving amplitude<sup>10, 11</sup>. In semiclassical treatment a chaotic operational regime is analyzed on phase space of dimensionless position and momentum  $x = \text{Re}(\alpha)$  and  $y = \text{Im}(\alpha)$ , where  $\alpha = \langle a \rangle$  is the oscillatory complex amplitude (see, Eq.(11)). Choosing  $x_0$  and  $y_0$  as an arbitrary initial phase-space point of the system at the time  $t_0$ , we define a constant phase map in the plane by the sequence of points at  $t_n = t_0 + (2\pi/\delta)n$ , where  $n = 0, 1, 2, \dots$ . This means that for any  $t = t_n$  the system is at one of the points of the Poincaré section.

The analysis show that for time scales exceeding the damping time,  $t \gg \gamma^{-1}$ , the asymptotic dynamics of the system is regular in the limits of small and large values of the modulation frequency, i.e.,  $\delta \gg \gamma$ ,  $\delta \ll \gamma$  and small or large amplitude of driving field  $f_1 \ll f_0$ ,  $f_1 \gg f_0$ . Fig. 1(c)

shows the results of numerical calculations of the classical maps, for the parameters chosen in the range of chaos, i.e.  $f_0 \approx f_1$  and  $\delta \geq \gamma$ . As we see, the figure clearly indicates the classical strange attractor with fractal structure that is typical for a chaotic dynamics.

It should be mentioned, that the Wigner function is one of the quantities that allows to observe chaos in quantum theory. The nonstationary Wigner function is written as for the state vector  $|\psi(t)\rangle$ .

$$W(\alpha, t) = \frac{2}{\pi^2} \exp(-2|\alpha|^2) \int d^2\beta \langle -\beta | \psi(t) \rangle \langle \psi(t) | \beta \rangle \exp(-2(\beta\alpha^* - \beta^*\alpha)) \quad (8)$$

We apply the QSD to determine Wigner functions for the quantum states of a driven anharmonic oscillator during time evolution. For this, we use the well-known expression for the Wigner function in terms of the matrix elements  $\rho_{nm} = \langle n | \rho | m \rangle$  of the density operator in the Fock state representation:

$$W(r, \theta) = \sum_{n,m} \rho_{nm}(t) W_{mn}(r, \theta). \quad (9)$$

Here:  $(r, \theta)$  are the polar coordinates in the complex phase-space plane,  $x = r \cos \theta$ ,  $y = r \sin \theta$ , while the coefficients  $W_{mn}(r, \theta)$  are the Fourier transform of matrix elements of the Wigner characteristic function:

$$W_{mn}(r, \theta) = \begin{cases} \frac{2}{\pi} (-1)^n \sqrt{\frac{n!}{m!}} \exp i(m-n)\theta (2r)^{m-n} \\ \exp(-2r^2) L_n^{m-n}(4r^2), \quad m \geq n, \\ \frac{2}{\pi} (-1)^m \sqrt{\frac{m!}{n!}} \exp i(m-n)\theta (2r)^{n-m}, \\ \exp(-2r^2) L_m^{n-m}(4r^2), \quad n \geq m. \end{cases} \quad (10)$$

It is remarkable that there is a correspondence between contour plots of the Wigner function and the Poincaré section. This point is illustrated on the Fig. 1, where the Wigner function Fig. 1(a), its contour plot, Fig. 1(b) and Poincaré section, Fig. 1(c) are presented for the same parameters. Note, that the Wigner function is a quasidistribution in phase space averaging an ensemble of quantum trajectories obtained for a define time moment while Poincaré section is the distribution for time intervals: it is constructed by fixing points in phase space at a sequence of periodic moments. What we can conclude from their correspondence is the fact, that the quantum distribution in phase space corresponds on the form to the semiclassical distribution but for big numbers of time intervals. As it is seen, the Poincaré



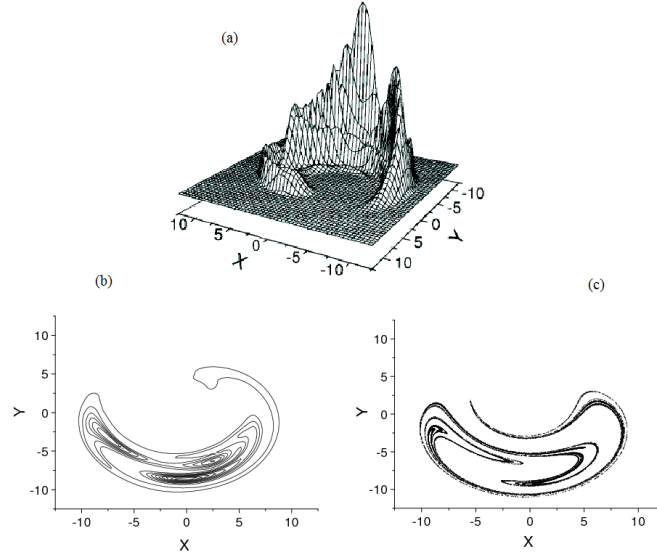


Fig. 1. The Wigner function (a) and its contour plot (b) averaged over 3000 trajectories. The Poincaré section (c) (20000 points plotted at times of the constant phase for the same parameters). In both cases, the dimensionless parameters are in the range of chaos, i.e.  $\chi/\gamma = 0.1$ ,  $\Delta/\gamma = -15$ ,  $f_0/\gamma = f_1/\gamma = 27$ ,  $\delta/\gamma = 5$ .

section has fine fractal structure while Wigner function contour plot has not. This is due to the Hiesenberg uncertainty relations which prevent sub-Plank structures in phase space.

#### 4. Scaling invariance in dissipative chaos

In this section the scaling invariance for the case of chaotic dynamics is considered on the base of anharmonic oscillator with time-dependent driven force. In the classical limit the system is described by the following equation of motion for the dimensionless amplitude:

$$\frac{d\alpha}{dt} = -\frac{\gamma}{2}\alpha - i(\Delta + \chi(1 + 2|\alpha|^2))\alpha - i(f_0 + f_1 \exp(-\delta t)). \quad (11)$$

This equation is invariant for the scaling transformation of complex amplitude  $\alpha = \lambda\alpha$  if the other parameters transforms like:  $\Delta \rightarrow \Delta' = \Delta + \chi(1 - 1/\lambda^2)$ ,  $\chi \rightarrow \chi' = \chi/\lambda^2$ ,  $f \rightarrow f' = \lambda f$ ,  $\gamma \rightarrow \gamma' = \gamma$ . This scaling property of the classical equation for the chaotic dynamics leads to

the symmetry of strange attractors: they have the same form in the phase space and differ from each other only in scale. This fact is demonstrated in the Fig. 2.

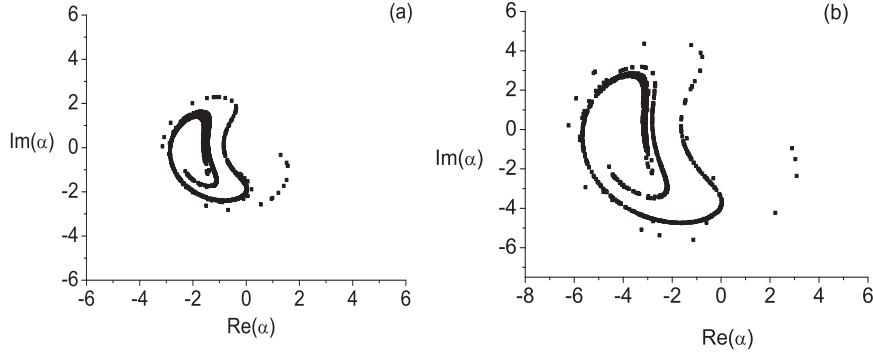


Fig. 2. The Poincaré section for the following parameters:  $\Delta/\gamma = -15$ ,  $\chi/\gamma = 2$ ,  $f_0/\gamma = 5.8$ ,  $f_1/\gamma = 4.9$ ,  $\delta/\gamma = 2$ , 2((a)); for the scaled  $\lambda = 2$  parameters 2((b)). The Poincaré sections are generated for time evaluation 5000 force periods.

Strictly speaking the quantum system does not obey the same scaling invariance as classical one. An analysis of scaling invariance from the point of view of quantum-statistical theory has been performed<sup>12</sup>. It was shown that such parameter scaling occurs for wider ranges of the parameters, but for not large values of the parameter  $\chi/\gamma$ , where system displays strong quantum properties.

Now we use the scaling arguments considering stochastic dynamic of a single trajectory in this way: to investigate chaos we use Poincaré section based on evolution of a single quantum trajectory, Eq.5. The Poincaré section is obtained by recording  $(Re(\alpha_\xi), Im(\alpha_\xi))$  at time intervals of  $2\pi/\delta$ , where  $\xi$  indicates the stochastic variable and  $\alpha_\xi$  is obtained from Eq. 5. Our goal is to analyze the scaling invariance on the base of this quantity. On the other side we present results that relies on quantum-classical correspondence.

In this direction, we consider the specific parameters for which DAO is in the vicinity of chaotic behavior determined classically. That means, if the parameters are slightly tuned in this range the transition from chaotic to regular dynamics might be realized. As we have realized above the dynamics of the system is chaotic in the range of parameters  $f_0 \simeq f_1$  and  $\delta \geq \gamma$ . Particularly, it is demonstrated on the base of the semiclassical Poincaré section

the system exhibits chaotic dynamics for  $f_0/\gamma = f_1/\gamma = 5.8$ ,  $\Delta/\gamma = -15$  and  $\delta/\gamma = 2$  in classical treatment. As analysis shows for the considered parameters the system dynamics continues to be chaotic till  $f_1/\gamma = 4.9$  (Fig.2), while chaotic dynamics becomes regular for  $f_1/\gamma = 4.8$ . Thus, we examine Poincaré section in quantum trajectory started from the regular regime, for the parameter  $f_1/\gamma = 4.8$ . The results of calculations are presented in Fig. 3 for the parameters:  $\Delta/\gamma = -15$ ,  $\chi/\gamma = 2$ ,  $f_0/\gamma = 5.8$ ,  $\delta/\gamma = 2$ ,  $f_1/\gamma = 4.8$ . As we see, for the scaled parameter  $\lambda = 1$  the Poincaré section is distributed stochastically but approximately exhibits localization in two ranges (Fig. 3(a)); its shape does not coincide with Poincaré section (Fig.2(c)). For the case of  $\lambda = 2$ , points of the Poincaré section on a trajectory are distributed chaotically, however, unlike to the previous case  $\lambda = 1$ , here an correspondence between both shapes take place. This likeness become more obvious for the case of  $\lambda = 3$  (Fig. 3(e)).

It is important to note that in the semi-classical treatment all cases  $\lambda = 1, 2, 3$  correspond to regular regime as it is expected due to scaling invariance. Another situation is realized in the quantum treatment. For  $\lambda = 1$  the system seems to be in regular regime. This statement is also confirmed by calculation of the Wigner function. The calculations shows that for such parameters the Wigner function has two-peak structure indicating that the regime of bistability is realized. If we increase the scaling parameter the resulted Poincaré section's shapes in a quantum trajectory in their forms are coincided with Poincaré sections in semiclassical treatment. So we found the parameters for which the system in classical treatment has regular dynamic while in quantum treatment its dynamic is chaotic.

The results on mean excitation numbers are presented on Fig. 3(b, d, f). As we see, for  $\lambda = 1$ , the oscillatory excitation numbers varies from 1 to 4 and thus the system is in deep quantum regime. The level of quantum noise is comparatively sufficient and chaos cannot exhibit itself on Poincaré section. But for scaled parameters  $\lambda = 2, 3$  the excitation numbers increase and varies up to 40 (Fig. 3(d,f)). For these cases the ranges of variation are much enough to exhibit a chaotic type structures.

Note, the usefulness of scaling procedure. It allows us to analyze classically analogy regimes for various groups of the parameters. In particular, increasing scaling parameter of the system we can investigate quantum-classical correspondence.

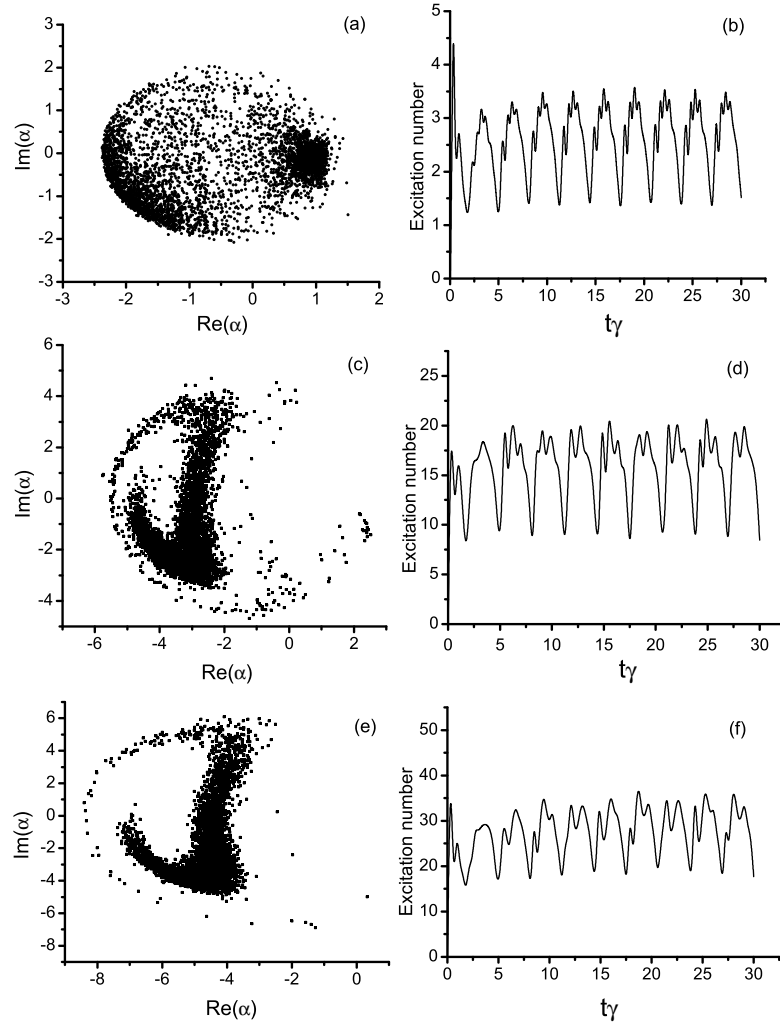


Fig. 3. The Poincaré section calculated on the base of a single trajectory for the following parameters:  $\Delta/\gamma = -15$ ,  $\chi/\gamma = 2$ ,  $f_0/\gamma = 5.8$ ,  $f_1/\gamma = 4.8$ ,  $\delta/\gamma = 2$ , (Fig. 3 (a)); the excitation number for the same parameters (Fig. 3(b)). Figs. 3(c) and 3(d) corresponds to scaled  $\lambda = 2$  parameters. Figs. 3(e) and 3(f) corresponds to scaled  $\lambda = 3$  parameters. The Poincaré sections are generated for time evaluation 5000 force periods.

## 5. Quantum interference assisted by chaos

It is well assessed that in the case of unitary dynamics, without any losses, an anharmonic oscillator leads to sub-Poissonian statistics of oscillatory excitation number, quadratic squeezing, and superposition of macroscopically distinguishable coherent states. The dissipation and decoherence lead usually to losses of these effects. In this section, we have numerically studied the phenomena at the overlap of chaos, dissipation, and quantum effects for the time-dependent nonlinear model. It was recently shown<sup>11, 12, 13</sup> that physical systems based on this model have a potential for generation of high-degree sub-Poissonian light as well as for the observation of quantum-statistical effects and quantum interference that accompanied by chaotic dynamics. Here we concentrate on studies of quantum interference. We have pointed out that the time modulation of the oscillatory parameters, which are the strength of third-order nonlinearity or the amplitude of the driving force, leads to formation of the quantum-interference patterns in phase space in over transient regimes, for the definite time intervals exceeding the transient dissipation time.

It is well known that the phase-space Wigner distribution function can simply visualize nonclassical effects including quantum-interference. For example, a signature of quantum interference is exhibited in the Wigner function by non-positive values. In this section the numerical results of the nonstationary Wigner functions in chaotic regimes of AHO are presented and discussed.

It should be noted that the most of investigations of the quantum distributions of oscillatory states, including also modes of radiations, have been made for the steady-state situations. The simplicity of Kerr nonlinearity allows to determine the Wigner function of the quantum state under time evolution due to interaction. In this sense, we note the main peculiarity of our paper in comparison with above noted important inputs. In this paper, we calculate the Wigner functions in an over transient regime,  $t \gg \gamma^{-1}$ , of the dissipative dynamics, however, we consider time-dependent effects which appear due to the time-modulation of the oscillatory parameters.

Below we investigate the Wigner functions for time-modulated nonlinearity. Note that the dynamics of the system with time-modulated nonlinear strength AHO is chaotic in the ranges:  $\delta \geq \gamma$  and  $\chi_0 \simeq \chi_1$  and for negative detuning. As shows analysis, controlling transition from the regular to chaotic dynamics can be realized through the intermediate ranges of bistability by varying the strength  $\chi_1$  of the modulation processes in the ranges from  $\chi_1 \ll \chi_0$  to  $\chi_1 \leq \chi_0$ . The results of the ensemble averaged

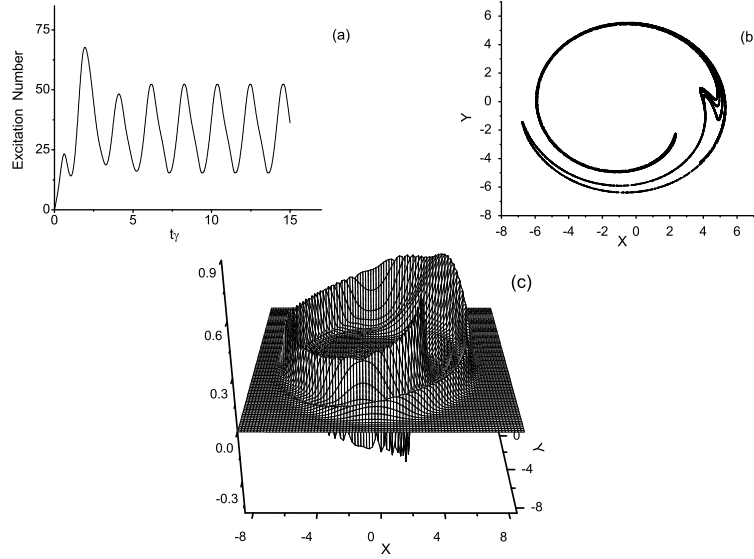


Fig. 4. The mean excitation number (a); the *Poincaré* section (b) ( $\approx 20000$  points) for the dimensionless complex amplitude  $\alpha$ , plotted at times of the constant phase  $\delta t_k = 2\pi k$  ( $k = 0, 1, 2, \dots$ ), when the maximal interference pattern on the Wigner function (c) is realized, for the case of time-modulated nonlinearity  $\chi(t)$ . The parameters are in the range of chaos:  $\Delta/\gamma = 5$ ,  $\chi(t)/\gamma = 0.2(1 + 0.75 \sin(\Omega t))$ ,  $\Omega/\gamma = 3$ ,  $f/\gamma = 10$ .

numerical calculation of the mean excitation number, the Poincaré section and the Wigner function are shown on the Figs. 4 respectively. The mean excitation number of the driven AHO versus dimensionless time is depicted in Fig. 4 (a). In contrast to the semiclassical result its quantum ensemble counterpart (see, Fig. 4(a)) has clear regular periodic behavior for time intervals exceeding the characteristic dissipation time, due to ensemble averaging. The Fig. 4(b) clearly indicates the classical strong attractors with fractal structure that are typical for a chaotic *Poincaré* section. Thus, the Wigner function (Fig. 4(a)) reflects the chaotic dynamics, its contour plots in the  $(x, y)$  plane are similar to the *Poincaré* section. However, the Wigner functions have regions of negative values for the definite time intervals. The example depicted on Fig. 4(a) corresponds to time intervals  $\gamma t_k = 6 + \frac{2\pi k}{\delta} \gamma$  ( $k = 0, 1, 2, \dots$ ), for which the mean excitation number reaches a macroscopic

level, i.e.,  $n = 52$ . The interference pattern is destroyed as the time modulation is decreased. Indeed, it is shown<sup>33, 34</sup> that for oscillatory mode of driven anharmonic oscillator including dissipation the Wigner function is positive in all phase space.

## 6. Conclusion

In summary, we have discussed dissipative chaos answering what is the counterpart of the semiclassical Poincaré section in quantum treatment. We have presented a type of nonstationary systems showing chaotic dynamics and intrinsically quantum properties which are modelled by a driven dissipative anharmonic oscillator with time-dependent parameters. The connection between quantum and classical treatments of chaos has been realized by means of a comparison between strange attractors on the semiclassical Poincaré section, the shapes of the Poincaré section on a single quantum trajectory and the contour plots of the Wigner functions. We have analysed the borders of validity of scaling invariance for quantum dissipative chaos and we have demonstrated realization of long-lived quantum interference assisted by chaotic dynamics for over transient regime and for the macroscopic level of oscillatory excitation numbers.

## Acknowledgments

This work was supported by NFSAT/CRDF grant UCEP-02/07 and ISTC grants A-1517 and A-1606.

## References

1. M. C. Gutzwiller, *Chaos in Classical and Quantum Systems* (Springer-Verlag, Berlin, 1990); *Quantum Chaos, Quantum Measurement*, edited by P. Citanovic, I. Percival, and A. Wzba (Kluwer, Dordrecht, 1992); K. Nakamura, *Quantum Chaos, A New Paradigm of Nonlinear Dynamics*, Vol. 3 of Cambridge Nonlinear Science Series (Cambridge University Press Cambridge, 1993); *Quantum Chaos*, edited by G. Casati and B. Chirikov (Cambridge University Press, Cambridge, 1995); F. Haake, *Quantum Signatures of Chaos* (Springer-Verlag, Berlin, 2000).
2. E. Ott, M. Antonsen, Jr., and J.D. Hanson, *Phys. Rev. Lett.* **53**, 2187 (1984); T. Dittrich and R. Graham, *Ann. Phys. (N.Y.)* **200**, 363 (1990).
3. A. Peres, in *Quantum Chaos: Proceedings of the Adriatico Research Conference on Quantum Chaos*, edited by H. A. Cerdeira et al. (World Scientific, Singapore 1991); A. Peres, *Quantum Theory: Concepts and Methods* (Kluwer, Dordrecht, 1993); R. Schack and C.M. Caves, *Phys. Rev. Lett.* **71**, 525 (1993).

4. W. H. Zurek and J. P. Paz, Phys. Rev. Lett. **72**, 2508 (1994); **75**, 351 (1995); S. Habib, K. Shizume, and W. H. Zurek, *ibid.* **80**, 4361 (1998); J. Gong and P. Brumer, Phys. Rev. E **60**, 1643 (1999).
5. W. H. Zurek, Nature (London) **412**, 712 (2001).
6. N. Gisin and I. C. Percival, J. Phys. A **25**, 5677 (1992); **26**, 2233 (1993); **26**, 2245 (1993); I. C. Percival, Quantum State Diffusion (Cambridge University Press, Cambridge, (2000).
7. T. P. Spiller and J.F. Ralph Phys. Lett. A **194**, 235 (1994).
8. T.A. Brun, I.C. Percival, and R. Schack, J. Phys. A **29**, 2077 (1996); T. Bhattacharya, S. Habib, and K. Jacobs, Phys. Rev. Lett. **85**, 4852 (2000).
9. H. H. Adamyan, S. B. Manvelyan, and G. Yu. Kryuchkyan Phys. Rev. A **63**, 022102 (2001).
10. H. H. Adamyan, S. B. Manvelyan, and G. Yu. Kryuchkyan Phys. Rev. E **64**, 046219 (2001).
11. G. Yu. Kryuchkyan and S. B. Manvelyan, Phys. Rev. Lett. **88**, 094101 (2002);
12. G. Yu. Kryuchkyan and S. B. Manvelyan, Phys. Rev. A **68**, 013823 (2003).
13. T. G. Gevorgyan, A. R. Shahinyan, G. Yu. Kryuchkyan Phys. Rev. A. **79**, 062905, (2009).
14. I. Kozinsky, H. W. Ch. Postma, O. Kogan, A. Husain and M. L. Roukes, Phys. Rev. Lett. **99**, 207201 (2007).
15. H. W. Ch. Postma, I. Kozinsky, A. Hussian, and M. L. Roukes, Appl. Phys. Lett. **86**, 223105 (2005).
16. X. M. H. Huang, C. A. Zorman, M. Mehregany, and M. L. Roukes, Nature (London) **412**, 496 (2003); K. C. Schwab and M. L. Roukes, Phys. Today **58**, N7, 36 (2005).
17. A. N. Cleland and M. R. Geller, J. App. Phys. **92**, 2758 (2002); A. N. Cleland and M. R. Geller, Phys. Rev. Lett. **93**, 070501 (2004).
18. I. Katz, A. Retzker, R. Straub, and R. Lifshitz, Phys. Rev. Lett. **99** 040404 (2007).
19. E. Buks, E. Segev, S. Zaitsev, B. Abdon, and M. P. Blencowe, Europhys. Lett., **81** 10001 (2008).
20. R. Almog, S. Zaitsev, O. Shtempluck, and E. Buks, App. Phys. Lett. **90**, 013508 (2007); J. S. Aldridge and A. H. Cleland, Phys. Rev. Lett **94**, 156403 (2005).
21. R. Almog, S. Zaitsev, O. Shtempluck, and E. Buks, Phys. Rev. Lett. **98**, 078103 (2007).
22. E. Babourine-Brooks, A. Doherty, G. J. Milburn, quant-ph/ 0804.3618v1, (2008).
23. M. P. Blencowe, Phys. Rep. **395** 159 (2004); T. J. Kippling and K. J. Vahala, Opt. Expr. **15**, 17172 (2007); M. Aspelmeyer and K. Schwab, New J. Phys. **10**, 095001 (2008).
24. A. E. Kaplan, Phys. Rev. Lett. **48**, 138 (1982).
25. D. Enzer and G. Gabrielse, Phys. Rev. Lett. **78**, 1211 (1997); G. Gabrielse, H. G. Dehmelt, and W. Kells, *ibid.* **54**, 537 (1985).
26. M. Rigo, G. Alber, F. Mota-Furtado, and P. F. OMahony, Phys. Rev. A **55**, 1665 (1997); **A58**, 478 (1998).



27. F. Diedrich, J. C. Berquist, W. M. Itano, and D. J. Wineland, *Phys. Lett.* **62**, 403 (1989); D. J. Wineland, C. Monroe, W. M. Itano, D. Leibfried, B. E. King and D. M. Mekhot, *J. Res. Natn. Inst. Standt. Technol.* **103**, 259 (1998).
28. S. Mancini and P. Tombesi, *Phys. Rev.* **A52**, 2475 (1995).
29. A. Imamoglu, H. Schmidt, G. Woods, and M. Deutsch, *Phys. Rev. Lett.* **79**, 1467 (1997); M. J. Werner and A. Imamoglu, *Phys. Rev. A* **61** 011801(R) (1999); M. Fleischhauer A. Imamoglu, and J. P. Marangos, *Phys. Mod. Phys.* **77**, 633 (2005).
30. P. Bermel, A. Rodriguez, J. D. Joannopoulos, and M. Soljacic, *Phys. Rev. Lett.* **99**, 053601 (2007).
31. F. G. S. L. Brandao, M. Hertmann, and M. B. Plenio, *New J. Phys.* **10**, 043010 (2008).
32. Q. A. Turchette , C. J. Hood, W. Lange, H. Mabuchi, and H. J. Kimble, *Phys. Rev. Lett.* **75**, 4710 (1995); K. Nemoto, W. J. Munro, *Phys. Rev. Lett.* **93**, 250502 (2004); W. J. Munro, K. Nemoto and T. P. Spiller, *New J. Phys.* **7**, 137 (2005); J. Lee, M. Paternostro, C. Ogden, Y. W. Cheong, S. Bose and M. S. Kim, *New J. Phys.* **8**, 23 (2006).
33. K. V. Kheruntsyan *J. Opt. B: Quantum Semiclass. Opt.* **1**, 225 (1999).
34. G. Yu. Kryuchkyan and K. V. Kheruntsyan *Opt. Commun* **120**, 132 (1996).
35. K. V. Kheruntsyan D. S. Krahmer, G. Yu. Kryuchkyan and K. G. Petrossian, *Opt. Commun* **139**, 157 (1997).
36. P. D. Drummond and D. F. Walls, *Phys. Rev. A* **23** 2563 (1981).